Dissociation Free Energy Profiles for Water and Methanol on TiO_2 Surfaces

Verónica M. Sánchez,*,† Julie A. Cojulun,†,‡ and Damián A. Scherlis*,†

Departamento de Química Inorgánica, Analítica y Química Física/INQUIMAE, Facultad de Ciencias Exactas y Naturales, Universidad de Buenos Aires, Ciudad Universitaria, Pab. II, Buenos Aires (C1428EHA) Argentina, and Department of Mechanical and Aerospace Engineering, University of California—Irvine, Irvine, California 92697

Received: March 15, 2010; Revised Manuscript Received: April 27, 2010

The umbrella sampling methodology is applied in the framework of density functional theory and Car−Parrinello molecular dynamics simulations to obtain the free energy profiles for the dissociation of methanol and water on stoichiometric TiO_2 surfaces. In particular, we study the dissociation of water on rutile (110) and anatase (101), and the dissociation of the O−H and C−O bonds of methanol on anatase (101). We discuss the reaction free energies and activation barriers of these processes in the light of experiments and previous simulations at zero temperature. The entropic contribution to the reaction free energy is found to be positive for the dissociation of water and negative for the dissociation of methanol.

I. Introduction

For many reasons, titanium dioxide surfaces are among the most widely studied to date. This material has found applications in heterogeneous catalysis, coatings, solar cells, sensors, and, more recently, the design of biomaterials.[1–3] Furthermore, TiO_2 is inexpensive and undefective faces are relatively easy to prepare, which has made of it a prototype oxide in surface science research. In response to the huge interest in understanding surface reactivity of titania, starting in the mid-90's, density functional theory (DFT) in periodic boundary conditions has been employed to investigate the interaction and the reaction pathways of small molecules on a variety of TiO_2 faces. First-principles simulations have addressed the adsorption of inorganic species as water,[4–11] oxygen,[12] or hydrogen peroxide,[6] and also of organic compounds such as methanol, formaldehyde, or acetic and formic acids.[6,13–19] All of this work has contributed priceless information regarding the structure and the energetics of adsorption processes on TiO_2. The vast majority of these studies, however, have involved static calculations at zero temperature. Only in very few cases, finite temperature statistical sampling or special pathway-scanning techniques have been employed to obtain reaction free energies or kinetic barriers.

The most abundant polymorphs of titanium dioxide are rutile and anatase, with the (110) and the (101) surfaces being in each case the most stable. As such, rutile (110) and anatase (101) have concentrated much of the experimental and computational efforts invested in elucidating TiO_2 reactivity. According to DFT calculations by Harris and Quong, water adsorbs molecularly on rutile (110) below monolayer coverage.[9] The barrier to dissociation was assumed to be very small, as suggested by TPD (temperature programmed desorption) experiments showing that a fraction of the molecules belonging to the first layer dissociated at 160 K.[20] In fact, spontaneous dissociation had been previously reported in molecular dynamics trajectories at 500 K.[4] In later works, the internal energy barrier was computed on the same surface trough different approaches. Lindan and Zhang applied a constrained optimization scheme to find an energy barrier of 8.3 kcal/mol at a coverage of half a monolayer.[10] Oviedo et al., on the other hand, estimated a value of 6.9 kcal/mol using the nudged elastic band (NEB) method.[11] For methanol on rutile (110), static DFT calculations rendered dissociative adsorption more favorable than molecular adsorption by just 4 kcal/mol.[13] On anatase (101), electronic structure studies indicate that molecular adsorption predominates for both water and methanol.[5,16,21,22] Barrier to dissociation was studied for the case of water on an oxygen vacancy: a free energy barrier of 2.8 kcal/mol was obtained through the blue moon ensemble method.[8]

In this work, we combine Car−Parrinello molecular dynamics simulations with the umbrella sampling methodology to investigate the dissociation free energy profile of water and methanol on clean faces of TiO_2. In the framework of umbrella sampling, the exploration of phase space relies on a large number of molecular dynamics simulations, each one biased toward a particular state along the reaction path.[23] Examples abound regarding the utilization of this method to investigate chemical reactions in vacuum or in biological environments; however, we are unaware of previous applications to study the reactivity of interfaces. In particular, we consider the dissociation of water on rutile (110) and anatase (101), and for this last surface we also examine the dissociation of methanol through the rupture of the O−H and the C−O bonds. These processes are schematized in Figure 1. Reaction and activation free energies are the most relevant thermodynamic variables involved in chemical processes at constant temperature and pressure, because they determine the equilibrium and the kinetic parameters ruling the reaction. Yet, they are not trivially accessible by computer simulation, nor by experiments, and so they are seldom reported in the literature. Thereafter, our purpose is 2-fold. On the one hand, we intend to establish the values of the kinetic barriers and the reaction free energies for key processes in the context of the surface chemistry of TiO_2. On the other, we seek to assess how the energies obtained at 0 K, which amount to the majority of the published data, compare to the free energies collected at room temperature.

II. Computational Methods

All calculations were performed using DFT in periodic boundary conditions as implemented in the Quantum-Espresso

* To whom correspondence should be addressed.
† Universidad de Buenos Aires.
‡ University of California—Irvine.

10.1021/jp102361z
Published on Web 06/16/2010

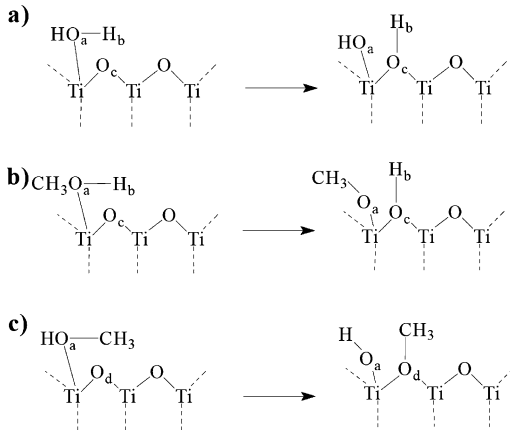

Figure 1. Schematics representing the dissociation of (a) the O−H bond in water, (b) the O−H bond in methanol, and (c) the C−O bond in methanol.

package.[24] The Kohn−Sham orbitals and charge density were expanded in plane-waves basis sets up to a kinetic energy cutoff of 25 and 200 Ry, respectively. The Perdew−Wang (PW91) approach to the exchange-correlation energy[25,26] and Vanderbilt ultrasoft pseudopotentials[27] were adopted to compute the total energies and forces. Geometry optimizations were performed at the Born−Oppenheimer approximation, whereas molecular dynamics simulations were carried out within the Car−Parrinello method[28] using a Nóse Hoover thermostat at 300 K and a time step of 0.17 fs. Reciprocal space sampling was restricted to the Γ -point.

The anatase (101) surface was represented by a (2 × 2) slab four layers deep, whereas in the case of rutile (110), a (2 × 1) surface made of four layers of atoms was adopted. The supercell dimensions were 7.55 × 10.20 × 22.00 Å^3 for anatase and 6.01 × 6.48 × 24.00 Å^3 for rutile, both of them containing a total of 48 atoms excluding the adsorbates.

Application of the umbrella sampling approach requires a specific reaction path to be decided in advance.[23] This is usually straightforward for simple dissociation processes as those considered here. Along the biased molecular dynamics, the total energy E_{tot} was calculated according to the umbrella sampling scheme[23]

$$E_{tot} = E_{KS} + \frac{1}{2}k_u(\xi - \xi_0)^2 \qquad (1)$$

where E_{KS} is the energy for the unperturbed Hamiltonian (in this case the standard Kohn−Sham energy) and ξ is the reaction coordinate, which was defined specifically for each reaction (see next section). A series of molecular dynamics runs were performed for different values of ξ_0, covering the full pathway between reactants and products, in steps of 0.1−0.2 Å. The force constant k_u was tuned for appropriate sampling. A histogram was produced for each value of ξ_0, reflecting the (logarithmic) probability distribution of ξ along the whole trajectory. For each ξ_0, simulation times varying from 1 to 4 ps were necessary to get converged distributions, depending on k_u and the width of the spanned ξ space. Every histogram was then weighted by the exponential factor $e^{(-1/2)k_u(\xi - \xi_0)^2}$, to extract a piece of curve representing the free energy around ξ_0. Finally, the free energy profile was constructed by matching these pieces corresponding to adjacent values of ξ_0.[23,29]

III. Results and Discussion

A. Water Dissociation on Rutile (110) and Anatase (101). On rutile (110), energy minimizations yield the molecular state of water as the most stable. In agreement with previous results,[9] we find it is only 3.4 kcal/mol below the dissociated state, in which a proton is transferred to a bridge oxygen atom on the surface (see Figure 1a). This difference is close to the chemical accuracy of density functional theory, and it has been shown that is quite sensitive to surface coverage and slab thickness.[9] For those reasons, the adsorption mode of water on rutile (110) has been a matter of controversy in the literature until recently.[7,9] To investigate the free energy associated with the break of the O−H bond, we proposed the following reaction coordinate:

$$\xi = |\mathbf{r}(O_a) - \mathbf{r}(H_b)| - |\mathbf{r}(O_a) - \mathbf{r}(O_c)| \qquad (2)$$

where $\mathbf{r}(O_a)$, $\mathbf{r}(O_c)$, and $\mathbf{r}(H_b)$ refer, respectively, to the spatial coordinates of the water oxygen atom, the bridge oxygen atom of the surface, and the transferred proton (Figure 1a). The first term on the right-hand side of eq 2 induces the rupture of the O_a-H_b bond consistently with the increase of the reaction coordinate, whereas the second term directs the hydroxyl group toward the bridge atom O_c. With this choice, which of course is not unique, ξ varies from around −1.6 to −0.9 Å as the reaction evolves from the molecular (reactant) to the dissociative (product) state. This kind of reaction coordinate has been already employed in the study of simple reaction pathways through restrained minimization techniques[30] or umbrella sampling simulations.[31,32] Figure 2 displays the free energy as a function of ξ. The dissociation free energy is only 0.4 kcal/mol, which gives an equilibrium constant of nearly 0.5. In turn, the activation free energy to dissociate the proton turns out to be 2.7 kcal/mol or ca. 4 kT, significantly lower than the barriers estimated previously on the basis of zero temperature calculations.[10,11] Our results suggest that molecular and dissociated water would coexist on the undefective (110) surface, exhibiting a fast dissociation-recombination behavior at room temperature. Such conclusions are consistent with TPD spectra[20] and with spontaneous dissociation observed during molecular dynamics at 500 K.[4] A positive entropic contribution can be estimated from the difference between the reaction energy at zero temperature (assuming it to be a reasonable approximation to the reaction enthalpy and disregarding its temperature depen-

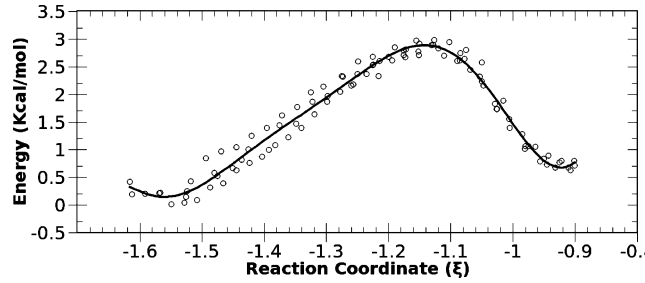

Figure 2. Free energy profile for the dissociation of H_2O on rutile (110).

TABLE 1: Reaction Internal Energies (Δ*E*), Reaction Free Energies (Δ*G*), Activation Free Energies (Δ*G*$^{\#}$), and Entropies (Δ*S*) Involved in the Dissociation of Water and Methanol

	Δ*E*, kcal/mol	Δ*G*, kcal/mol	Δ*G*$^{\#}$, kcal/mol	Δ*S*, J K^{-1} mol^{-1}
rutile (110)$H_2O \rightarrow$ OH + H	3.4	0.4	2.7	42
anatase (101)				
$H_2O \rightarrow$ OH + H	9.7	6.7	10.5	42
$CH_3OH \rightarrow CH_3O + H$	7.3	8.5	13.6	−17
$CH_3OH \rightarrow CH_3 + OH$	6.2	7.2	60.3	−14

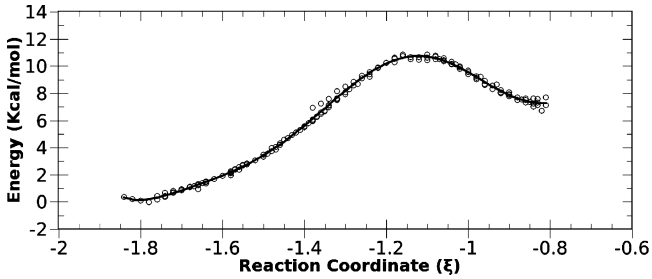

Figure 3. Free energy profile for the dissociation of H_2O on anatase (101).

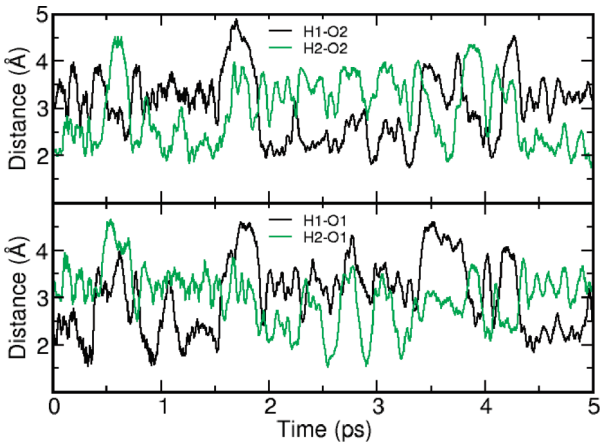

Figure 4. Time evolution of the distances from the hydrogen atoms H1 and H2 of the H_2O molecule to the oxygen atoms O1 and O2 on the surface, according to Car−Parrinello molecular dynamics of water on anatase (101). H-bonding interactions H1−O1 and H2−O2 alternate every few picoseconds with H1−O2 and H2−O1.

dence) and the free energy at 300 K. This data is collected in Table 1.

In the case of water on anatase (101), two H-bonds arise between the adsorbed molecule and the two closest bridge oxygen atoms of the surface. The internal energy turns out to be 9.7 kcal/mol lower for molecular adsorption than for the dissociative path. A similar structure and energy difference were found by Vittadini et al.[5] In Figure 3, the reaction coordinate corresponding to reactants is slightly more negative than in rutile, because the distance from H_2O to the bridge atom in anatase is longer. Umbrella sampling analysis yields a reaction free energy of 6.7 kcal/mol (Figure 3 and Table 1). This leads to a dissociation entropy of 42 J K^{-1} mol^{-1}, in remarkable agreement with the value obtained for rutile (110). In fact, in both surfaces the reactions involve breaking and forming of the same bonds. The activation energy to go from the dissociated to the molecular state is also larger than on rutile (3.8 kcal/mol versus 2.3 kcal/mol), reflecting the longer distances between the surface sites in the (101) face.

Inspection of the trajectories at 300 K reveals that most of the time the water molecule maintains simultaneously the two hydrogen bonds evinced in the geometry optimization. This behavior is illustrated in Figure 4, where the distances between the H_2O protons and the oxygen sites on the TiO_2 surface are monitored during 5 ps of dynamics. In the lower panel the identity of the oxygen atoms is inverted with respect to the upper panel. At the beginning of the simulation, water hydrogen atoms labeled H1 and H2 are bonded to atoms O1 and O2 of the interface, respectively. These bonds tend to subsist with some interruptions during the first 1.5 ps of dynamics, and then the molecule flips and the interactions are exchanged, to produce

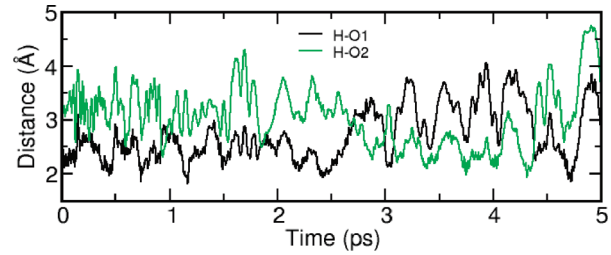

Figure 5. Time evolution of the distances from the hydrogen atoms of the methanol molecule to the oxygen atoms O1 and O2 on the surface, according to Car−Parrinello molecular dynamics of water on anatase (101). Hydrogen bonds form alternatively with O1 and O2.

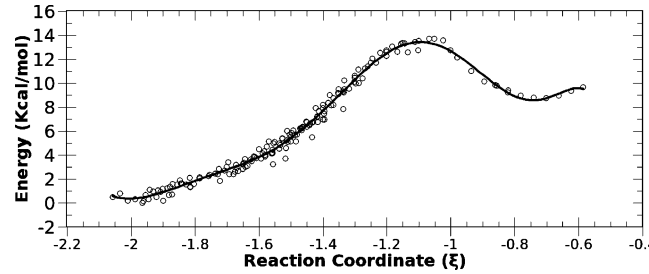

Figure 6. Free energy profile for the dissociation of methanol across the O−H bond on rutile (110).

bonds H1−O2 and H2−O1. Finally, at around 4.5 ps, the original connectivity is restored.

B. Methanol Dissociation on Anatase (101). The same reaction coordinate as introduced in eq 2 was used to examine dissociation of the O−H bond in methanol on the anatase surface. In this case, $\mathbf{r}(O_a)$ represents the position of the methanol oxygen atom. Table 1 shows that the internal reaction energy is slightly lower than for the dissociation of water on the same surface. This result is consistent with the larger proton acidity in methanol as compared to water, and is in agreement with previous calculations.[16]

The molecular dynamics simulations show that the OH group forms short-lived H-bonds rapidly alternating between two equidistant oxygen atoms of the surface. Figure 5 depicts the evolution of the interatomic distances between the proton and such oxygen atoms at 300 K. It can be seen that the molecule spends most of the simulation time H-bonded to either oxygen site: as soon as the distance to one of the O atoms increases, the other decreases.

From the thermodynamical analysis, ΔG turns out to be larger than ΔE (Figure 6 and Table 1), and so conversely to the case of water, we find a negative dissociation entropy for this reaction. We note that, in spite of being a dissociative process, the number of chemical bonds remains constant when evolving from reactants to products, and therefore the sign of ΔS is not an obvious question. Even so, the difference in the sign of ΔS for the dissociation of water in comparison to methanol is certainly intriguing, since in both cases a O−H bond is broken and a proton is transferred to a bridge oxygen site of the surface. As will be shown below, the entropy change for the rupture of methanol across the C−O bond is also negative. These results suggest that the methanol adsorbed on the surface, at variance with H_2O, exhibits an excess molecular entropy (in comparison with the dissociated species), which is lost regardless of the dissociation mechanism. The source of this entropy might be attributed to the rotation of the methyl group: this mode is lost upon dissociation, since the radicals CH_3−O or CH_3 are more strongly bound to the surface. We recall, as discussed above, that for both water and methanol there are two accessible,

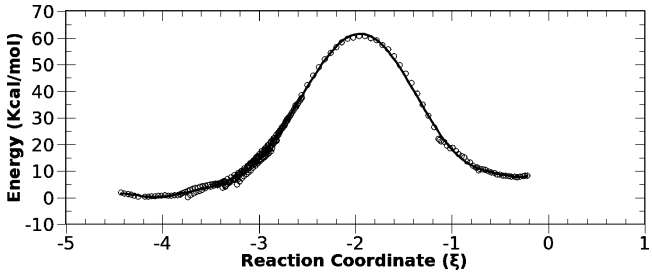

Figure 7. Free energy profile for the dissociation of methanol across the C−O bond on anatase (101).

degenerate H-bonded stable configurations, which are visited at intervals of 1−2 ps. This itineracy of the hydroxyl moiety might involve an entropic contribution which is lost with the molecular rupture, but should be equally present in both adsorbates.

Alternatively, we have considered the dissociation of methanol through breaking the C−O bond. To this end, a reaction coordinate depending on the positions of four nuclei was chosen:

$$\xi = |\mathbf{r}(O_a) - \mathbf{r}(C)| - |\mathbf{r}(O_d) - \mathbf{r}(C)| - |\mathbf{r}(O_a) - \mathbf{r}(Ti)| \quad (3)$$

where $\mathbf{r}(O_a)$, $\mathbf{r}(C)$, $\mathbf{r}(O_d)$, and $\mathbf{r}(Ti)$ refer, respectively, to the spatial coordinates of the methanol oxygen atom, the methanol carbon atom, the bridge oxygen atom of the surface, and the five-coordinate titanium atom to which the hydroxyl is bound (Figure 1). Given the large activation barrier to break the $C-O_a$ bond (see below), the use of a reaction coordinate analogous to that in eq 2 implemented for the dissociation of the O−H bond, led in the present case to the rupture of the $Ti-O_a$ link, which offers a lower dissociation barrier. For this reason, it was necessary to include the $Ti-O_a$ distance in the choice of ξ, to force the $C-O_a$ breaking while preserving the $Ti-O_a$ bond. This reaction coordinate assumes that $C-O_a$ dissociation proceeds concertedly with the formation of the $C-O_d$ bond. Under this definition, ξ is approximately −4.0 Å for reactants and −0.5 Å for products.

Table 1 indicates that the internal and free energy differences for this reaction are comparable to (or slightly smaller than) those found when the O−H bond is broken. However, the barrier to dissociation is huge, of nearly 60 kcal/mol (Figure 7), due to the strength of the C−O bond that needs to be disrupted. The formation of a new C−O link with the surface energetically compensates, to some extent, the original one; but the activation barrier could never be surmounted in the absence of a catalytic agent.

As a final remark, it is worth noting that the (negative) entropic term for this reaction is surprisingly close to that corresponding to the dissociation across the O−H bond (−14 versus −17 J K^{-1} mol^{-1}). This reinforces the notion that most of the entropy change in both reactions comes from the disappearance of the methanol molecule.

IV. Conclusions

In this study we have calculated activation and free energies for the dissociation of water and methanol on perfect titania surfaces. In spite of the relevance of these processes in the context of surface reactivity of TiO_2, to the best of our knowledge, estimates of the free energies involved had not been reported before. Our results show, consistently with previous simulations at zero temperature, that on anatase (101) molecular adsorption of water and methanol are strongly favored. Spontaneous dissociation of these molecules on anatase would only be feasible in the presence of defects, as demonstrated by other authors.[8] In the case of rutile (110), the stability of the dissociated and the molecular forms of water becomes comparable. Thus, both are likely to coexist on the surface, displaying a fast, reversible interconversion.

For all the cases examined in this study, it was found that the entropic term contributed less than 3 kcal/mol, in absolute value, to the reaction free energies at 300 K. This result constitutes, to some extent, and at least for these kind of simple dissociative processes, a validation of the widespread use of energies at 0 K to assess the adsorption mode at room temperature. The entropic effect, however, might play a role to the point of altering the relative trends predicted by the computations at zero temperature. This is the case of CH_3OH and H_2O on anatase (101): the ΔE values suggest methanol should dissociate more easily than water, which turns out to be false when the entropy is considered.

The umbrella sampling technique proved to be an efficient, valuable tool to compute activation barriers and reaction free energies for dissociative processes at interfaces. Whereas this technique exhibits the disadvantage that tentative pathways must be provided beforehand, this requirement has little impact on elementary reactions as those proposed here, where simplicity rules out the chance of alternative routes. Yet, we do not imply the application of the umbrella sampling method is restricted to these kind of basic processes. With the exploration of a proper set of reaction coordinates judiciously selected, we envision it could become an extremely useful instrument to look into many kinds of surface chemistry problems, from catalytic transformations to vacancy diffusion.

Acknowledgment. We express our gratitude to Dr. Nano Gonzalez Lebrero for sharing with us his experience on the subtleties of umbrella sampling. This work was supported by funding granted to D.A.S. by the Agencia Nacional de Promoción Científica y Tecnológica de Argentina (PICT 2007-2111) and by the University of Buenos Aires (UBACYT X490). V.M.S. acknowledges CONICET for a doctoral fellowship. J.A.C. acknowledges NSF-CHE-0755022 grant for her international REU experience in Argentina.

Supporting Information Available: All reaction coordinates, ξ_0, and force constants, k_u, utilized in the umbrella sampling simulations together with the histograms reflecting the probability distributions during the molecular dynamics runs. This material is available free of charge via the Internet at http://pubs.acs.org.

References and Notes

(1) Diebold, U. *Surf. Sci. Rep.* **2003**, *48*, 53.
(2) Henderson, M. A. *Surf. Sci. Rep.* **2005**, *46*, 1.
(3) Pang, C. L.; Lindsay, R.; Thornton, G. *Chem. Soc. Rev.* **2008**, *37*, 2328.
(4) Lindan, P. J. D.; Harrison, N. M.; Holender, J. M.; Gillan, M. J. *Chem. Phys. Lett.* **1996**, *261*, 246.
(5) Vittadini, A.; Selloni, A.; Rotzinger, F. P.; Grätzel, M. *Phys. Rev. Lett.* **1998**, *81*, 2954.
(6) Bates, S. P.; Kresse, G.; Gillan, M. J. *Surf. Sci.* **1998**, *409*, 336.
(7) Schaub, R.; Thostrup, P.; Lopez, N.; Lgsgaard, E.; Stensgaard, I.; Nrskov, J. K.; Besenbacher, F. *Phys. Rev. Lett.* **2001**, *87*, 266104.
(8) Tilocca, A.; Selloni, A. *J. Chem. Phys.* **2003**, *119*, 7445.
(9) Harris, L. A.; Quong, A. A. *Phys. Rev. Lett.* **2004**, *93*, 86105.
(10) Lindan, P. J. D.; Zhang, C. *Phys. Rev. B* **2005**, *72*, 075439.
(11) Oviedo, J.; Sánchez de Armas, R.; San Miguel, M. A.; Sanz, J. F. *J. Phys. Chem. C* **2008**, *112*, 17737.
(12) Tilocca, A.; Selloni, A. *ChemPhysChem* **2005**, *6*, 1911.

(13) Bates, S. P.; Gillan, M. J.; Kresse, G. *J. Phys. Chem. B* **1998**, *102*, 2017.
(14) Vittadini, A.; Selloni, A.; Rotzinger, F. P.; Grätzel, M. *J. Phys. Chem. B* **2000**, *104*, 1300.
(15) Käckell, P.; Terakura, K. *App. Surf. Sci.* **2000**, *166*, 370.
(16) Tilocca, A.; Selloni, A. *J. Phys. Chem. B* **2004**, *108*, 19314.
(17) Foster, A. S.; Nieminen, R. M. *J. Chem. Phys.* **2004**, *121*, 9039.
(18) Foster, A. S.; Gal, A. Y.; Nieminen, R. M.; Shluger, A. L. *J. Phys. Chem. B* **2005**, *109*, 4554.
(19) Köppen, S.; Langel, W. *Phys. Chem. Chem. Phys.* **2008**, *10*, 1907.
(20) Kurtz, R. L.; Stockbauer, R.; Madey, T. E.; Román, E.; de Segovia, J. L. *Surf. Sci.* **1989**, *218*, 178.
(21) Tilocca, A.; Selloni, A. *J. Phys. Chem. B* **2004**, *108*, 4743.
(22) Tilocca, A.; Selloni, A. *Langmuir* **2004**, *20*, 8379.
(23) Torrie, G.; Valleau, J. P. *J. Comput. Phys.* **1977**, *23*, 187.
(24) Giannozzi, P. *J. Phys.: Condens. Matter* **2009**, *21*, 395502; http://www.quantum-espresso.org/.
(25) Perdew, J. P.; Wang, Y. *Phys. Rev. B* **1992**, *45*, 13244.
(26) Perdew, J. P.; et al. *Phys. Rev. B* **1992**, *46*, 6671.
(27) Vanderbilt, D. *Phys. Rev. B* **1990**, *41*, 7892.
(28) Car, R.; Parrinello, M. *Phys. Rev. Lett.* **1985**, *55*, 2471.
(29) Frenkel, D.; Smit, B. *Understanding Molecular Simulation*, 2nd ed.; Academic Press: San Diego, CA, 2002.
(30) Sánchez, V. M.; Crespo, A.; Gutkind, J. S.; Turjanski, A. G. *J. Phys. Chem. B* **2006**, *110*, 18052.
(31) Bikiel, D. E.; Di Salvo, F.; González Lebrero, M. C.; Doctorovich, F.; Estrin, D. A. *Inorg. Chem.* **2005**, *44*, 5286.
(32) González Lebrero, M. C.; Estrin, D. A. *J. Chem. Theory Comput.* **2007**, *3*, 1405.

JP102361Z